5-2018

High Temperature Wide Bandgap Light Emitting Diodes for Harsh Environment Applications

Stephanie Sandoval

High Temperature Wide Bandgap Light Emitting Diodes for Harsh Environment Applications

An undergraduate honors thesis submitted in partial fulfilment
of the requirements for the degree of
Bachelor of Science in Electrical Engineering

by

Stephanie Sandoval

May 2018
University of Arkansas

Abstract

The need for high temperature, high power density power modules for applications such as electric vehicles and space exploration has driven the research into wide bandgap LEDs due to their potential operation at elevated temperatures. Wide bandgap LEDs offer an attractive solution due to properties such as high temperature tolerance, strong radiation hardness and good thermal conductivity. In this thesis, the electrical properties of GaN-on-SiC heterojunctions are studied as a precursor to an LED study, and the optical characterization of an InGaN/GaN MQW is reported. The GaN-on-SiC study revealed that these wide bandgap LEDs have linear sensitivity at high temperatures. The InGaN/GaN MQW PL results revealed that as the temperature increased, the bandgap decreased as well, thus affecting the overall intensity of the material. The results of this study indicate the feasibility of the integration of wide bandgap LEDs into high temperature power modules.

Acknowledgement

I would like to thank Dr. Chen for his wonderful mentorship, support, and encouragement he has offered me over the last 3 years of my undergraduate degree. If it was not for his mentorship and support, I would not have been able to gain such valuable research experience, nor would I have been able to complete this thesis. His encouragement has led me to pursue a graduate degree and he has made sure that I am well prepared to face that challenge.

I would also like to thank his graduate students, Syam Mudhusoodhanan and Abbas Sabar, for always making themselves available to me whether it was to help me with my research or answer my questions. They always made sure that I was on the right track and helped me immensely.

A special thank you goes to my family and boyfriend. Were it not for their love and encouragement, I would not have been able to complete my degree or have had the desire to pursue a higher education, much less this thesis. They have always been there for me when I needed them the most, and for that, I thank them.

Table of Contents

List of Figures

1.0 Introduction

Wide bandgap materials, such as gallium nitride (GaN) and silicon carbide (SiC) have great potential for harsh environment applications due to their unique properties such as high temperature tolerance, strong radiation hardness and good thermal conductivity. Wide bandgap semiconductor power devices have been demonstrated to outperform silicon (Si) power devices in many harsh environment applications [1]. However, wide bandgap optoelectronic materials and devices have not been fully explored yet.

By using wide bandgap semiconductor material as a light emitting diode (LED), one can achieve high reliability, stable operation at high temperatures (i.e., over 150^{o}C) and more compatibility with integrated circuits associated with wide bandgap materials. As a wide bandgap material, GaN shows great potential for high temperature LEDs.

The work that will be done with these GaN LED structures consists of device characterization such as electrical and optical analysis both in normal and extreme environments (i.e., elevated temperature up to 800K). With this characterization data, an understanding of the degradations or the failure of the LED devices as well as how they can be re-designed to be operated at high temperatures will be gained.

2.0 Background

2.1 Motivation

In 1965, Gordon E. Moore recognized that manufactures had been doubling the density of components per integrated circuit at regular intervals and would continue to do so well into the future. Now referred to as Moore's law, it is viewed as a reliable method to predict future trends and establish the pace for innovation and advancement [2]. An increase in performance in terms

of power efficiency, switching speed, thermal management, and power density is actively sought after in the development of scaled-down, high-temperature power modules [3].

High-temperature power modules are in high demand for use in harsh environments such as electric vehicles, energy storage, power grid, space exploration, aviation, deep oil drilling, and gas exploration [1], [4]. If these power modules can be scaled down and made more efficient, this could revolutionize industries such as automotive and power distribution since these systems would be more compact and easier to transport. High density, high temperature power modules become possible through the integration of wide bandgap semiconductor power devices due to their favorable properties such as high temperature tolerance, high critical field, high saturation velocity and low intrinsic carrier density [3].

For these power modules to properly operate in harsh environments, a reliable isolation system is required to protect low-power control circuitry from the high-power portion of the module. Isolation transformers are commonly used to isolate high voltage and high power; however, isolation transformers are bulky and heavy. A promising solution to replace isolation transformers are optocouplers. Optocouplers use optical coupling isolation, as seen in Figure 1, whereas isolation transformers use magnetic coupling isolation. Compared to isolation transformers, optocouplers are chosen due to their reduction in size, simplicity, ease of design, and ability to isolate high voltage from the logic input to the power output stage [5]. In order for optocouplers to completely replace isolation transformers, optocouplers must demonstrate operation capabilities at high temperatures without significant degradation or early failure. Due to high temperatures in the LED p-n junction and the optocoupler packaging material, the lifetime of a typical optocoupler can be substantially shortened if the operating temperature exceeds 250°C.

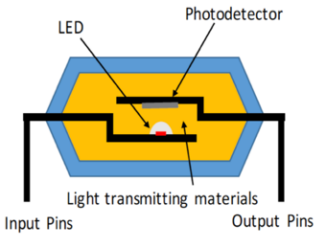

Figure 1. Cross-section of an optocoupler

In an optocoupler, the LED simply reads and converts an input current into an optical signal that is detected by the photodetector and is then transformed back into an output current [6]. In Figure 2, a simple optocoupler circuit with common collector configuration is shown. An input bias current flows through the LED causing it to emit light, with its intensity changing with the input current level. When the photodetector detects the light, current flows through a load resistor. At elevated temperatures, the LED injected current changes due to the increase in resistance value. Therefore, in order to provide constant injection current, an optocoupler with temperature compensation needs to be designed with the high-temperature LEDs as seen in Figure 3.

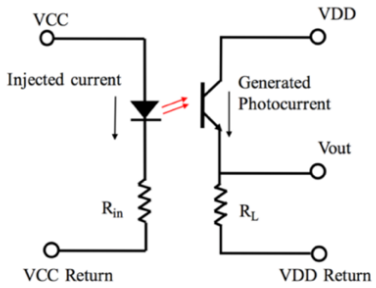

Figure 2. An optocoupler circuit with common collector configuration

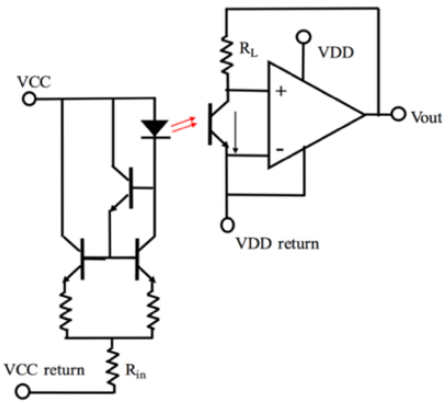

Figure 3. An optocoupler circuit with temperature compensation

The reliability of optocouplers is limited by the characteristics of the LED and packaging materials of the optocouplers [7]. Degradation of LEDs are accelerated at high operating temperatures which affects the temperature range of optocouplers. Limited by the operating temperature of the LED, current optocoupler technologies can operate at a maximum temperature of 100°C [6]. Therefore, LEDs with high operating temperature and long lifetime are needed to reliably operate optocouplers at high temperatures. As previously mentioned, wide bandgap LEDs are a promising choice to expand the operating range of these optocouplers due to the characteristics of wide bandgap semiconductors such as low performance-degradation at high temperatures, inherent radiation hardness, great thermal conductivity, and high breakdown field [4], [7].

2.1 Wide Bandgap Semiconductors

Wide bandgap semiconductors, such as SiC, are capable of operating at much higher temperatures than smaller bandgap semiconductors like Si. This has therefore fueled their development for harsh environment applications [1]. Traditional Si-based devices are not capable of operating at elevated temperatures above 250°C, especially when combined with high power, high frequency, and high radiation environments [4]. Due to their inherent material advantages

like higher thermal conductivity, higher breakdown voltage, larger energy bandgap, and comparable carrier mobility, wide bandgap semiconductors form the most attractive alternative to Si-based semiconductor devices [8]. For temperatures beyond the limits of Si, due to its wide bandgap, SiC can be used at temperatures over 600°C [7]. The limitations of Si are the strongest motivation for the shift to wide bandgap semiconductors in higher temperature applications [1].

There are a number of factors that limit the use of Si at high temperatures. With a bandgap of 1.12 eV, the Si p-n junction becomes depleted at high temperatures. The intrinsic carrier concentration of Si increases as the ambient temperature increases and as it approaches the doping concentration level, the p-n junction begins to behave as a resistor, not a diode, causing the transistors to lose their switching characteristics [1], [7]. From Figure 4, it is apparent that semiconductors with wide bandgaps (>3 eV), such as SiC and GaN, have much lower intrinsic carrier concentrations when compared to Si. By using wide bandgap semiconductors, conductivity loss from junction depletion can be avoided [1].

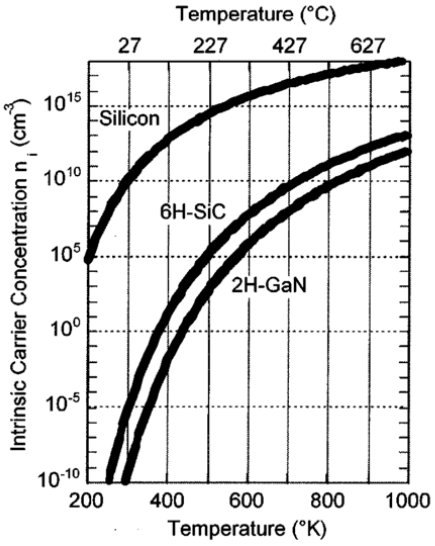

Figure 4. Semiconductor intrinsic carrier concentration versus temperature for silicon, 6H-SiC, and 2H-GaN[1]

Another limitation with narrow bandgap semiconductors is large leakage current. With increasing temperatures, there is an increase in leakage current through a reverse-biased p-n junction. For each 10°C rise in junction temperature, the leakage current approximately doubles. The increased junction leakage currents cause the power dissipation within the device to increase as well [7]. Power is often dissipated as heat and can significantly raise the temperature within a device well beyond ideal operating temperatures. Additionally, the increase in junction temperature can result in undesirable, unstable positive feedback loop of increasing temperature and power dissipation [1]. However, since wide bandgap semiconductors have low intrinsic carrier concentration, as seen in Figure 4, the leakage current levels are orders of magnitudes smaller than in Si [1]. Because of this, wide bandgap semiconductors devices are more capable of operating at high temperatures and could play a critical role in achieving high power electronics at temperatures beyond the limits of Si.

2.2 Semiconductor Diodes

One of the primary methods used to analyze diodes is through the analysis of its current-voltage (I-V) curve, similar to the curve seen in Figure 5 below. The I-V curve is broken down into three distinct regions: forward-bias, reverse-bias, and breakdown. Each of these regions are separately analyzed and each offer a unique perspective to the working mechanism of the device.

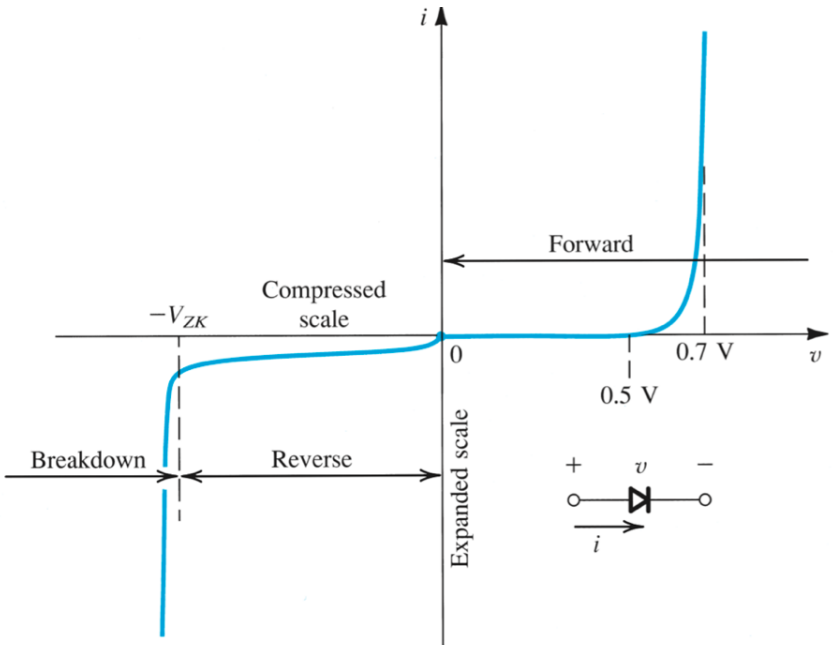

Figure 5. Detailed diode I-V characterization curve [9]

The forward-bias region of operation is the region where the terminal voltage is positive as seen in Figure 5. In this region, the I-V relationship is closely approximated by $i = I_S(e^{v/V_T} - 1)$, where V_T, the thermal voltage, is defined as $V_T = \frac{kT}{q}$ and k is Boltzmann's constant, T is temperature, and q is the electric charge. I_S, also known as the saturation current, is usually constant for a given diode at a given temperature. This saturation current is directly proportional to the cross-sectional area of the diode, thus the more area, the more current. However, I_S has a very strong dependence on temperature and doubles in value every for every 5°C rise in temperature [9]. Since I_S is a function of temperature, the forward I-V characterization curve is affected as temperature increases. Figure 6 below shows that at a constant current, the voltage drop decreases by approximately 2mV for every 1°C increase in temperature.

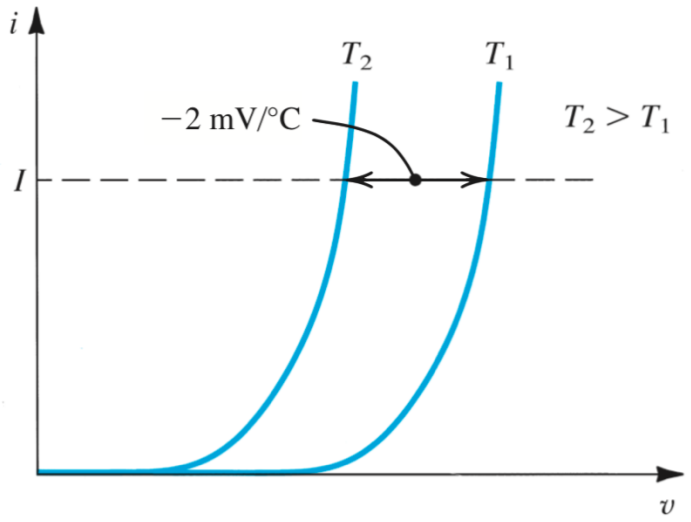

Figure 6. Temperature dependence of the diode forward characteristic curve [9]

The reverse-bias region is entered when the terminal voltage is negative as shown in Figure 5. In this region, the current in the reverse region is constant and equal to $-I_S$. A large part of this reverse current is due to the leakage current in the diode. The leakage currents are also proportional to the area, similar to the saturation current. These reverse currents also have a temperature dependence, however, these reverse currents double for every 10°C rise in temperature versus the 5°C rise in temperature seen in I_S [9].

Finally, the breakdown region of this I-V characteristic curve can be easily identified in Figure 5. The breakdown region is entered when the magnitude of the reverse voltage exceeds the threshold value for the diode in question. This crossing of the threshold is known as the breakdown voltage or the "knee" of the curve (V_{ZK} in Figure 5). As seen in the figure, this current increases rapidly over a very small voltage drop. This breakdown voltage is common and often not destructive, provided the power dissipated is limited as specified on a device datasheet [9].

Besides being able to extract data from each region of operations, the sensitivity of the device can also be extracted from the I-V characterization curve. To extract the sensitivity, the voltage-temperature curve must first be extracted at a constant current and then plotted. The

sensitivity of the device is then defined by the slope of the voltage-temperature curve. Later in this report, the sensitivity for some devices will be shown for a variety of different currents. Analyzing the sensitivity of the devices gives insight as to what occurs as the device size changes.

Overall, understanding what occurs in these regions allows the user to analyze the degradation or failure mechanisms that occur in these diodes.

2.3 Light Emitting Diodes

Simply put, an LED is a p-n junction that emits light when current is applied to it. When the p-n junction is forward-biased, charge carriers recombine as electrons cross from the n-region and recombine with the existing holes in the p-region as illustrated in Figure 7. When the recombination of electrons and holes occur, one of two things transpire, depending on the material. With direct bandgap materials, radiative recombination occurs when an electron in the conduction band falls into a hole found in the valence band. When this change occurs, energy is conserved by emission of photon, or light, as seen in Figure 8 [10]. With indirect bandgap material, non-radiative recombination occurs where recombination of electrons and holes does not result with the emission of a photon, or light, thus direct bandgap materials, such as GaN and indium gallium nitride (InGaN), are suitable for LEDs [10], [11]. When the p-n junction is reverse-biased, the LED does not emit light and can be damaged if the reverse voltage exceeds the breakdown voltage [12].

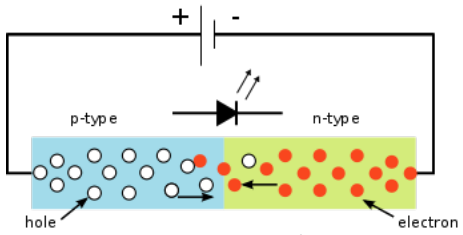

Figure 7. LED basic operation [12]

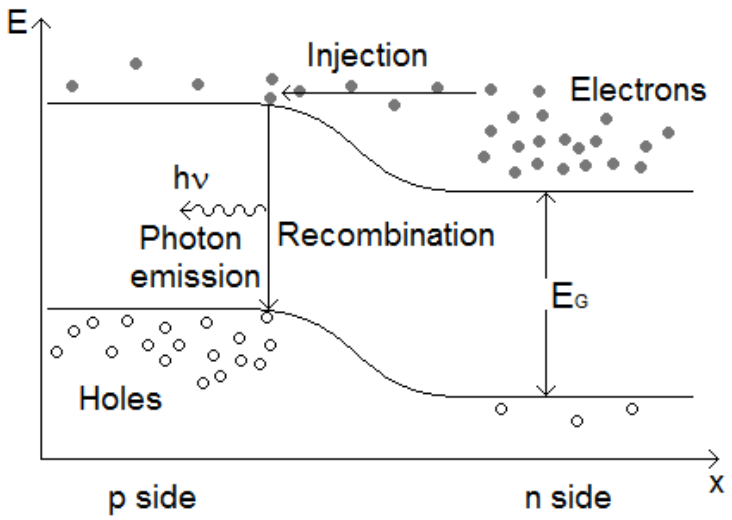

Figure 8. Recombination of electrons and holes within an LED [10]

Applications such as display backlighting, communications, medical services, and general illumination has driven the increased demand for LEDs. LEDs provide high performance with ultra-fast response time, a wider range of controllable color temperatures, a wider operating temperature range (-20°C to 85°C), and no low temperature startup problems [13]. Despite these advantages, at high power, thermal and mechanical loads can degrade and even destroy the package of LEDs by means of delamination's or cracks [14]. The operating temperature of LEDs is often limited by the melting point of the packaging material [7]. This issue is actively being studied and will need to be solved in order to develop these high temperature power modules.

For regular applications, LEDs with an operating range of -20°C to 85°C allow for flexibility of use, but for high-temperature power applications, an operating temperature of >350°C is ideal as mentioned previously. Wide bandgap semiconductors, such as GaN, can be used at temperatures over 600°C showing promise for the development of high temperature, high power LEDs. Overall, the combination of necessary material properties required to meet the high

temperature and high power application requirements can be found in wide bandgap semiconductors, thus motivating this study [1].

2.4 Characterization

2.4.1 Current-Voltage Characterization

In this study, GaN-on-SiC devices were tested under a vacuum using a cryostat to obtain their I-V characteristics. Using a vacuum with a mist eliminator, the sample was mounted on a hot stage with platinum resistor sensor in a temperature chamber as seen in Figure 9. These devices were tested on a temperature-controlled stage using a programmable SMU temperature controller, as shown in Figure 10, that provides accurate temperature cycling, precise and stable temperature ramping, and data acquisition functions over temperature ranging from 70K to 650K [15].

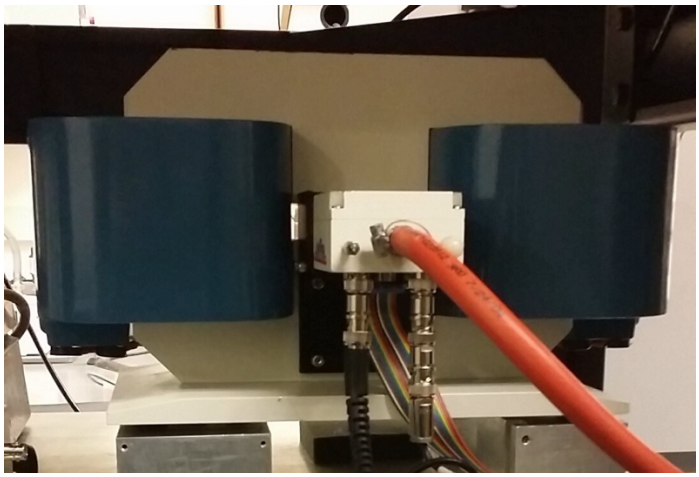

Figure 9. Temperature chamber

Figure 10. Temperature controller

2.4.2 Photoluminescence

One of the most common optical characterization techniques is photoluminescence (PL)[16]. This technique uses a laser to illuminate the structure with energetic photons to create electron-hole pairs in the structure. These excited charge carriers recombine and re-emit photons with the same energy as the bandgap of the LED. In other words, the light separates charge carriers within the band or impurity structure of a semiconductor and the recombination then produces characteristic emissions, giving insight to the semiconductor structure[17]. The resulting incident laser beam has a non-uniform, Gaussian profile [16].

PL is one of the most widespread optical characterization techniques and offers enormous capabilities for analysis of the device in question[17]. PL measurements allows the user to characterize several semiconductor properties such as the lattice alloy composition, lattice stress, presence and type of impurity and defect, surface behavior, interface behavior, and even allows for homogeneity mapping [17]. This measurement can be used to determine the energy gap of a semiconductor sample which is useful because it allows for an accurate measurement of, in this case, the percentage of indium (In) in the InGaN substrate from the position of the PL peak. For

most applications, it is important for this percentage to be accurately known [18]. Additionally, PL also detects the presence of impurities and crystalline defects which affect the material quality and device performance of the semiconductor[18].

For the PL measurements in this study, an InGaN/GaN multi-quantum well (MQW) sample was stressed at a temperature ranging from 10K to 800K using the set up as shown in Figure 11. The sample was loaded into the cryostat and a continuous wave laser of 395nm with pumping powers ranging from 1mW to 110mW was used for these PL measurements. This PL setup has a capability of stressing these devices from 10K to 800K and uses a 395nm laser specifically for wide bandgap material study.

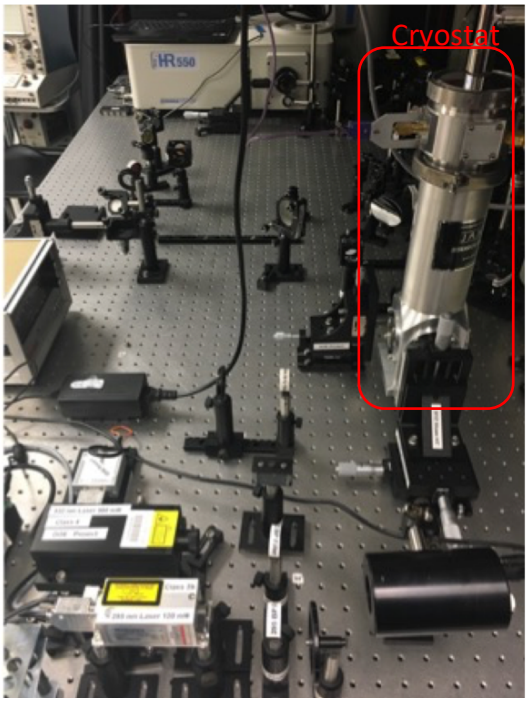

Figure 11. PL experimental setup

3.0 Experiment

3.1 GaN-on-SiC Heterojunction Diodes

GaN was grown by molecular beam epitaxy (MBE) on the Si face of a two inch, commercially available, n-type SiC substrate. With the thickness of the p-GaN layer being ~300 nm, p-type doping of the GaN was achieved using atomic magnesium at a level of ~10^{18} cm^{-3}. These heterojunction devices were fabricated using a concentric ring geometry with diameters ranging from 400µm to 1000µm as seen in Figure 12. Here, ohmic contacts were established on GaN using a Ni/Au multilayer film and on SiC using a single layer of Ni. A cross-sectional schematic of the fabricated GaN-on-SiC diode is shown in Figure 13. This document reports the characterization of three devices, a 400µm, 800µm, and a 1000µm device using the setup described in section 2.4.1.

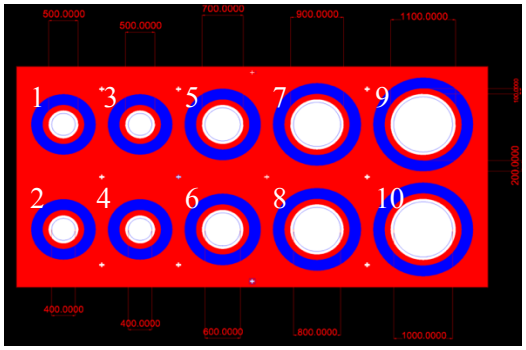

Figure 12. Fabricated heterojunction devices

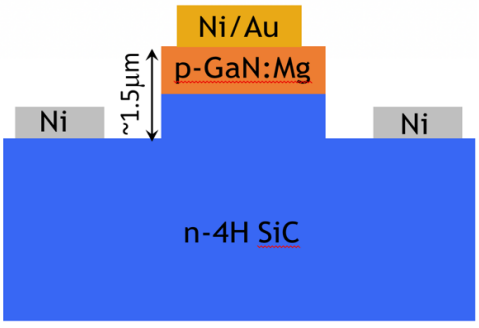

Figure 13. Cross-section schematic of fabricated GaN-on-SiC

In high power, high temperature applications, accurate knowledge of the junction temperature of a power semiconductor is critical to its thermal management. Optical methods, physically contacting methods, and on-die temperature sensing are some of the commonly used direct junction temperature sensing techniques [15]. These methods, however, are not suited for applications that require a high bandwidth temperature sensing due to their slow response [15]. An alternative to these methods is the fabrication of a small p-n junction diode on the same substrate as the power device. These diodes quasi-linear voltage-temperature characteristics can be utilized for temperature sensing [19] with a significantly faster dynamic response [20]–[22]. Therefore, for this study, ten GaN-on-SiC heterojunction diodes were characterized at high temperatures and analyzed for their use as temperature sensors.

3.2 InGaN/GaN Multi-Quantum Well

Within an optocoupler, it is important to be able to control the LED intensity in order to ensure the detector within the optocoupler can read the signal. At room temperature, this is easily achievable and easily controlled. However, at high temperatures, the LED performance is reduced, mainly due to the decrease in light intensity, thus a PL study is conducted in order to measure the intensity of the material as the temperature increases. Understanding how the intensity changes at a wide range of temperatures is important since at high temperatures, the detector still will need to be able to read the signal from the LED.

Optical characterization involving PL spectroscopy was conducted on an InGaN/GaN MQW structure grown on sapphire (001) in order to analyze the material intensity that occur at high temperatures. This was done using the PL setup as described in section 2.4.2. A cross-sectional schematic of this material is shown in Figure 14.

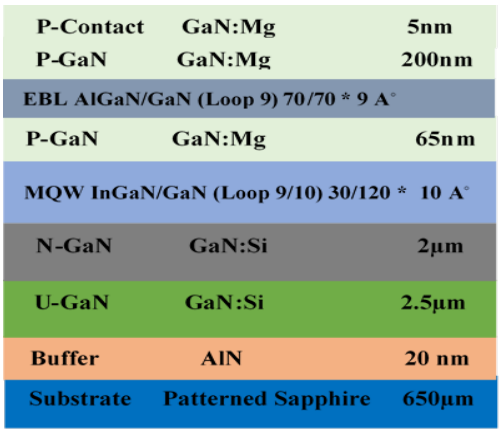

Figure 14. InGaN/GaN MQW cross section [23]

4.0 Results

4.1 High Temperature Current-Voltage Characterization of GaN-on-SiC Heterojunction Diodes

Before stressing these devices under high temperatures, initial I-V characteristic curves were taken at room temperature of all of the devices. Figure 15 below shows the initial I-V curves for two 400µm devices. It is observed that these two devices behave very similar to each other meaning that these devices can be reproduced to behave similarly. In figure 16, the initial I-V curves for each sized device is measured and plotted (400µm, 600µm, 800µm and 1000µm). As previously mention in section 2.2, as the area increases, so does I_S. This initial I-V curve shows that as the area increases from 400µm to 1000µm, the current at 2V also increases. These initial I-V curves at room temperature were conducted because it is important to know how a device behaves at room temperature in order to understand how they behave at elevated temperatures.

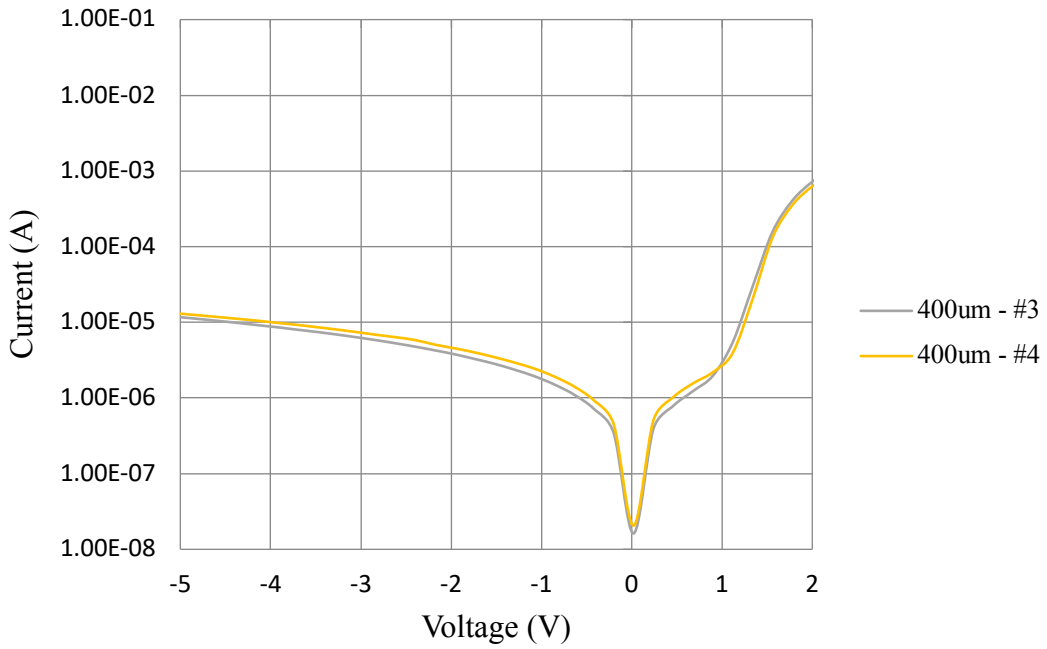

Figure 15. Initial forward and reverse I-V for two 400µm devices at room temperature

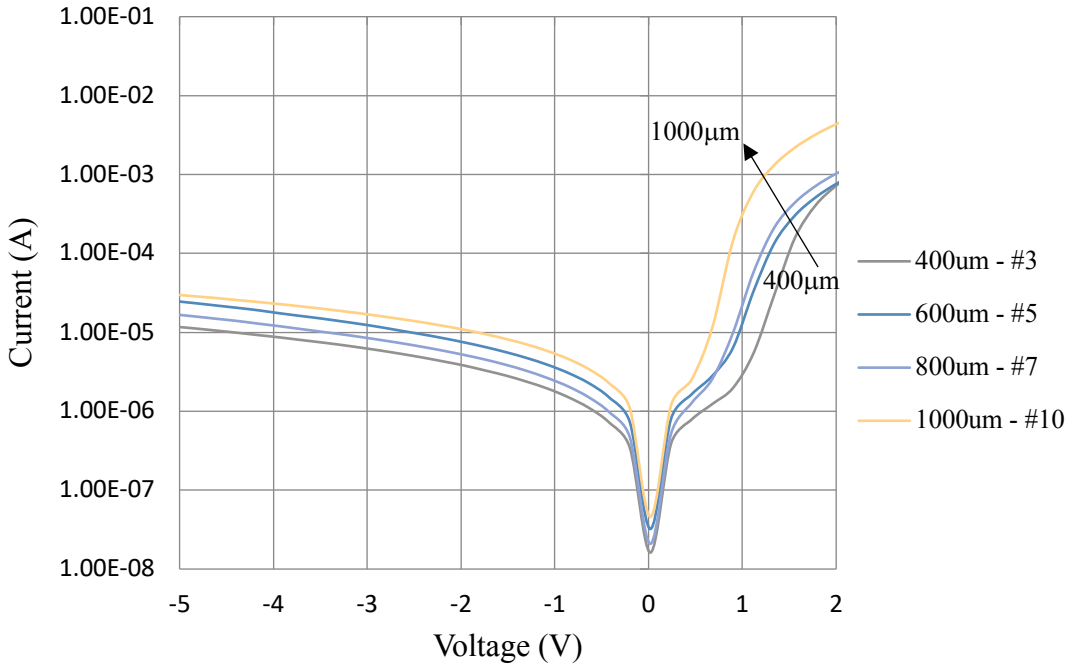

Figure 16. Initial forward and reverse I-V for all four size devices at room temperature

Figure 17 shows the measured I-V characteristics of the 400µm heterojunction diode stressed at temperatures ranging from 300K to 650K. The voltage was limited during these

measurements to avoid device degradation and damage. Figure 18 and 19 also shows the measured I-V characteristics of an 800µm and 1000µm device stressed at temperatures ranging from 300K to 500K. As shown in these I-V curves, all three devices follow a similar trend as temperature increases. The results obtained show that I_S has a temperature dependence consistent with that of Figure 6 in section 2.2. As the temperature increased, the voltage drop decreased in all three of these devices. Additionally, from the data obtained, it was shown that as the device cross-sectional area increased, the leakage current increased as well. This is consistent with the theory found in section 2.2. From these I-V curves, data such as the sensitivity, ideality factors, and saturation current can be extracted for further analysis. For this study, the sensitivity results were studied and analyzed for both devices and are presented below.

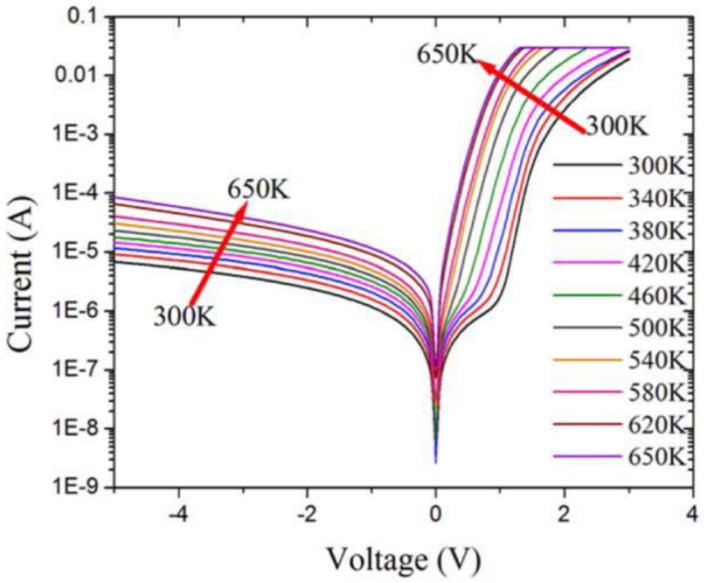

Figure 17. Forward and reverse I-V characteristics of a 400µm device [15]

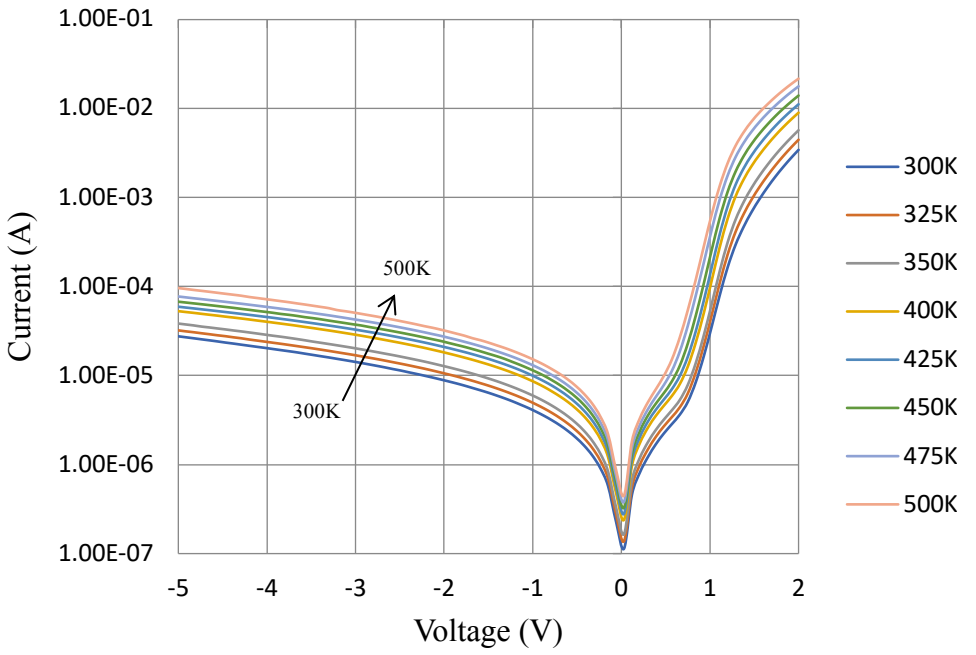

Figure 18. Forward and reverse I-V characteristics of an 800µm device

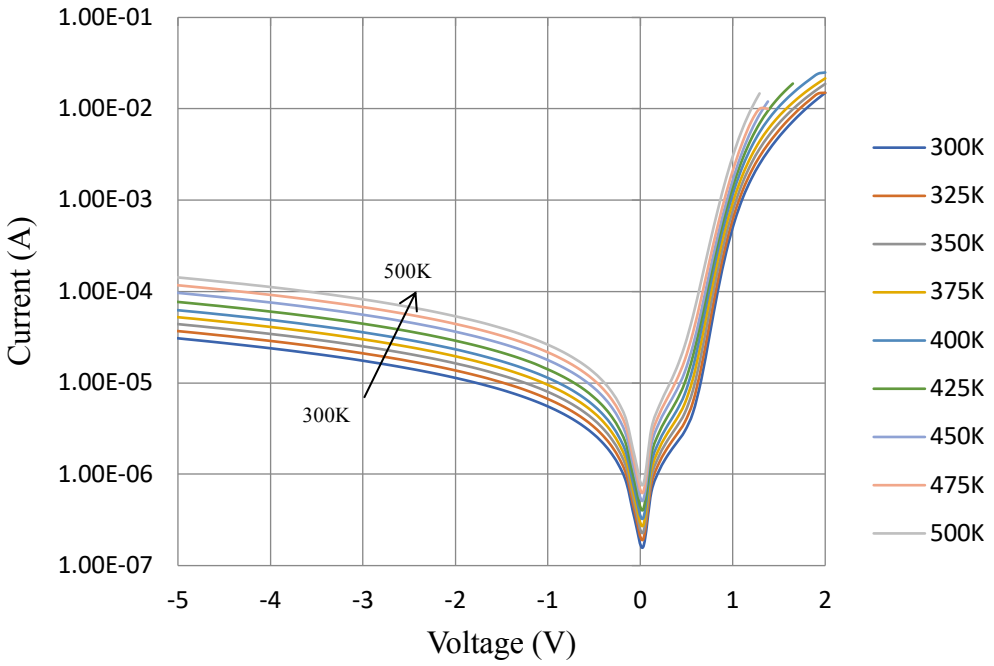

Figure 19. Forward and reverse I-V characteristics of a 1000µm device

4.2 Current-Voltage Characterization of GaN LED

Figure 20 below shows the I-V forward characteristic curve for a commercially available GaN LED. This LED device was stressed from 300K to 800K. It can be observed in this figure that as the temperature increased, the voltage drop across the LED also decreases. This is consistent with the theory found in Figure 6 in section 2.2 and with the heterojunction I-V curves seen in the previous section. These curves indicate that there are other thermal mechanisms dominating the shift in forward voltage and these mechanisms should be further explored. Furthermore, this measurement shows good, consistent linearity as the temperature increases. It is observed that as the temperature increases, the voltage drop consistently changes as well. When this stress was conducted, the device was not properly current limited resulting in a non-uniform curve at 800K. Despite this, linearity is observed. While this GaN LED was stressed to a much higher temperature than the heterojunctions, it can be observed that the they both behave similar to one another which show great potential for its overall use into high temperature optoelectronics. In order to fundamentally understand what occurs within the material and how it behaves at elevated temperatures, PL spectroscopy is conducted at the material level to analyze the intensity change in these harsh environments.

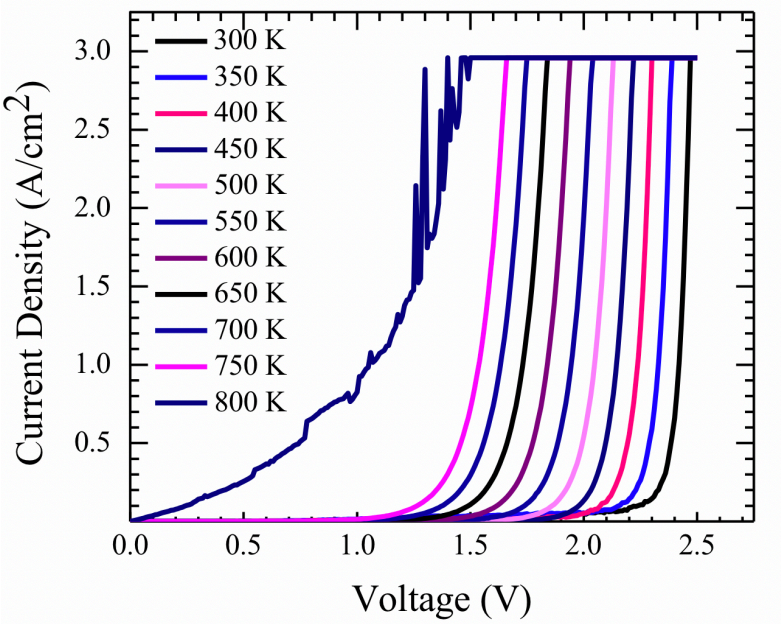

Figure 20. Commercially available GaN LED I-V characteristics curve

4.3 Sensitivity Characterization of GaN-on-SiC Heterojunction Diodes

Consistent with that of Figure 6 in section 2.2, the voltage drop across diode is linearly proportional to the temperature of the device when operated under constant current, similar to the operation of these heterojunctions and that of the GaN LED. The Shockley ideal diode equation expresses the ideal behavior of a diode assuming that all of the recombination does not occur in the junction. However, it is known that recombination occurs through many pathways and regions throughout the device, thus a non-unity ideality factor is introduced into the Shockley ideal diode equation to describe this recombination [15]. As a function of the applied bias-voltage, V, the expression for the diode current, I_D, is given by,

$$I_D = I_S\left(e^{\frac{qV}{nkT}} - 1\right) \qquad (1)$$

where q is the electric charge, k is the Boltzmann constant, T is the absolute temperature, and n is the ideality factor [15]. As expressed in this report, I_S, the reverse saturation current, is also temperature dependent and can be expressed as [24]

$$I = CT^r e^{-\frac{qV_g}{kT}} \qquad (2)$$

where C is a constant that depends on the geometric factors of the p-n junction diode, r is a process dependent parameter, and V_g is the bandgap equivalent voltage, with a temperature given by [15], [25]

$$V_g = V_g(0) - \frac{\alpha T^2}{\beta + T} \qquad (3)$$

Where $V_g(0)$ is the bandgap equivalent voltage at 0K and α and β are empirical constants. For $I_D >> I_S$, (1) can be simplified to

$$I_D = I_S\left(e^{\frac{qV}{nkT}}\right) \qquad (4)$$

By then substituting (2) into (4), solving for V yields

$$V = V_g + \frac{nkT}{q}(lnI_D - rlnT - lnC) \qquad (5)$$

Equation (5) shows that at a given current, the forward voltage drop is almost a linear function of temperature [15]. At very high temperatures, the effects of the nonlinear part of (5), rlnT, are very small as expressed in [15], [24]. The sensitivity results presented below, show the validity in these equations, showing a highly linear, non-varying sensitivity over a wide temperature range.

Figure 21 below shows the profiles of voltage versus temperature at 10μA, 50μA, 100μA, 500μA, and 1000μA that was extracted from the I-V curves for the 400μm device. Similarly, figures 22 and 23 show the profiles of voltage versus temperature at specific currents (10μA, 100μA, and 1000μA) that were also extracted from the 800μm and 1000μm device I-V curves and

plotted. Defined by the slope of the voltage-temperature curve, the sensitivity is displayed in the figure and in the table below the curve. As shown, the sensitivity slightly varies between 1.9 mV/K and 2.5 mV/K for a variety of current levels for the 800µm whereas the sensitivity slightly varied from 1 mV/K and 1.6 mV/K for the 1000µm device. The smaller 400µm device sensitivity also varied slightly from 2.19 mV/K to 2.25 mV/K. From the experimental results, the sensitivity displays a high degree of linearity which indicates great potential for their use as high temperature sensors to at least 500K [15]. Highly linear devices are important for their use as high temperature sensors and their applications into high power devices because due to their linearity, it is easy to predict their behaviors at a certain temperature without risking damaging the device.

I_D (μA)	10	50	100	500	1000
Sensitivity (mV/K)	2.19	2.22	2.22	2.21	2.25

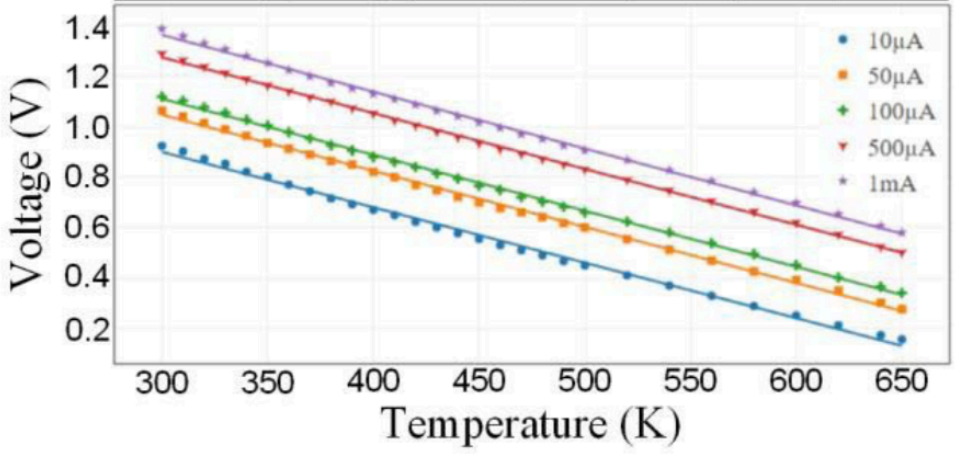

Figure 21. Forward voltage versus temperature characterization at different currents for a 400µm device. The table shows the sensitivity of each forward current [15].

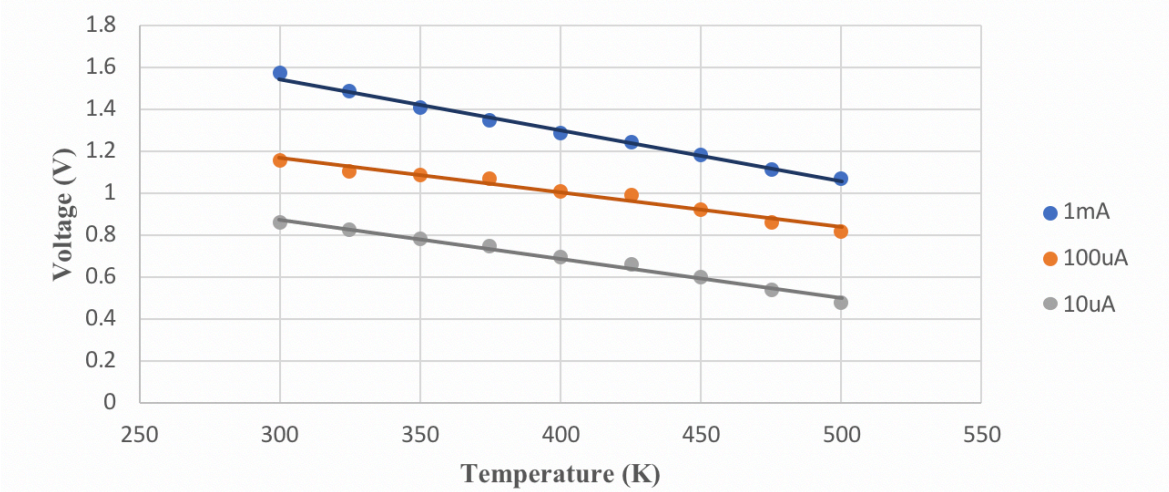

I_D (µA)	10	100	1000
Sensitivity (mV/K)	1.9	1.7	2.5

Figure 22. Forward voltage versus temperature characterization at different currents for an 800µm device. The table shows the sensitivity of each forward current.

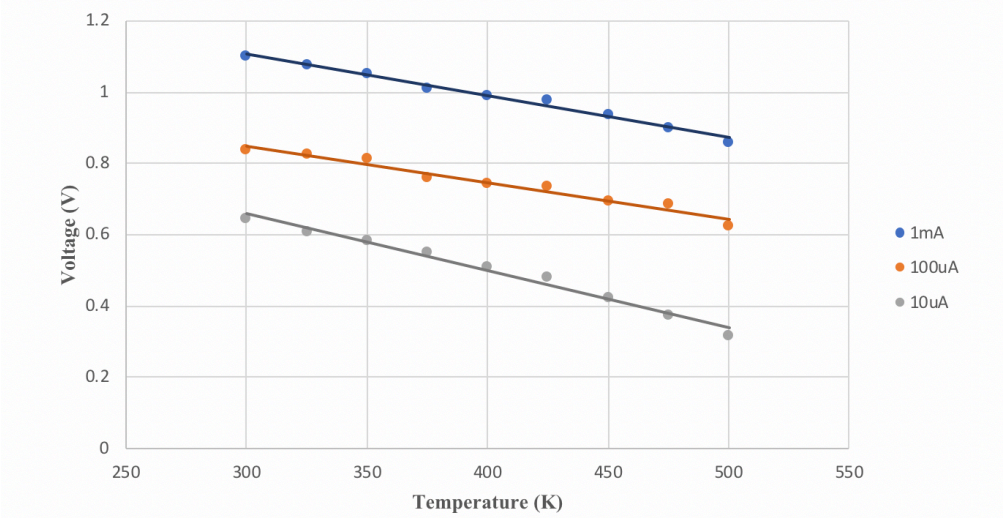

I_D (µA)	10	100	1000
Sensitivity (mV/K)	1.6	1	1.2

Figure 23. Forward voltage versus temperature characterization at different currents for a 1000µm device. The table shows the sensitivity of each forward current.

Similarly to the extraction of the sensitivity curves, the profiles of the forward voltage versus temperature for the 400µm, 600µm, 800µm and 1000µm devices were extracted from the

I-V curves for I_D = 10μA. In Figure 24 below, the dots represent the measured data with a fitted linear line. As can be seen, as the device area decreases, the sensitivity of the devices increases. This can be due to the lower material quality of the GaN grown on a commercially available, non-native SiC [15]. Overall, these devices have demonstrated excellent potential for high temperature sensors and applications.

Diameter (μm)	400	600	800	1000
Sensitivity (mV/K)	2.22	1.77	1.28	1.08

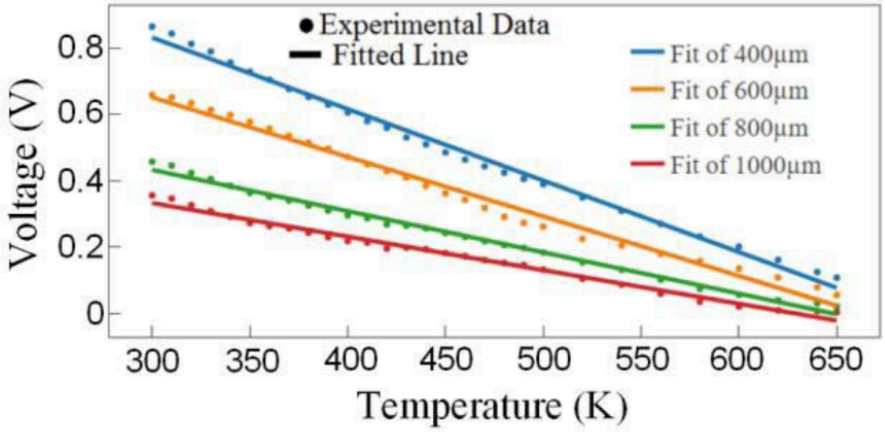

Figure 24. Forward voltage versus the temperature for the devices with different diameters. The table shows the sensitivity of different devices [15].

4.4 Optical Characterization of InGaN/GaN Multi-Quantum Well

Figure 25 shows the PL spectrum obtained when the sample was stimulated at temperatures ranging from 10K to 800K. It is observed that as the temperature increases, the peak decreases and shifts towards the right. This is known as redshift. This redshift shows that there is a reduction in bandgap as the temperature increases. From the peak positions in this spectrum, the bandgap energy can be calculated. While the material remains the same, the bandgap has been reduced. This shift in bandgap also changes the intensity of the material. As previously mentioned, it is important to know how the intensity of the material varies since the LED needs to be able to emit a strong enough signal for the detector to read within the optocoupler. Ultimately, the quantum

efficiency versus temperature will be studied. If there is a significant drop in quantum efficiency of the sample, then that shows that the sample in question is not appropriate for these applications. It is reported that the quantum efficiency of these InGaN/GaN MQW is to be around 44% quantum efficiency, indicating this MQW has great potential for high temperature optoelectronics [23].

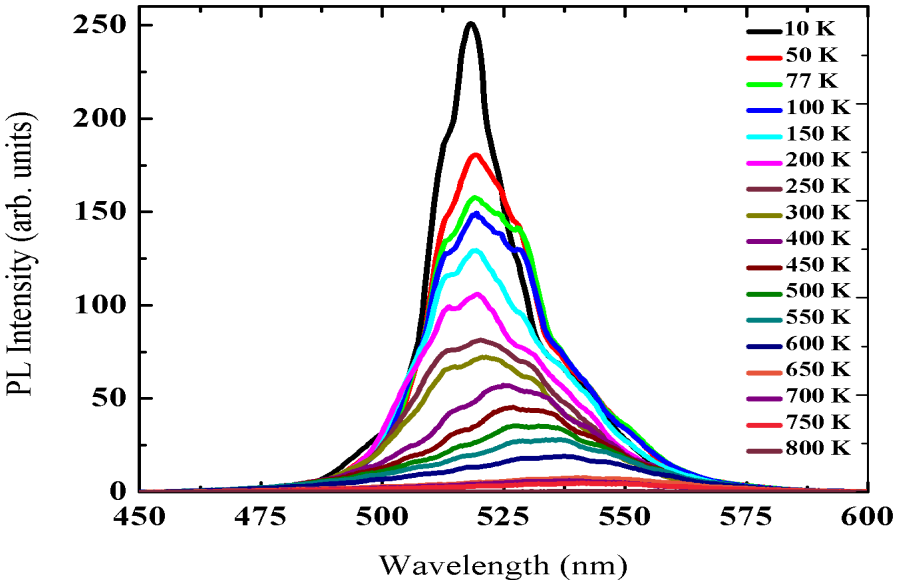

Figure 25. Temperature-dependent PL spectra of InGaN/GaN MQW [21]

5.0 Conclusion

5.1 GaN-on-SiC Heterojunction Diodes

The similarity of the I-V curves between 300K and 500K for all three devices in this study show that these GaN-on-SiC heterojunction diodes are highly linear and show great potential for their integration into high temperature power modules. As the operating temperature was increased from 300K to 500K, the saturation current increased by a relatively small amount. Similarly, the leakage current at a 5 V reverse bias increased with the cross-sectional area of the device, going from 96.5 μA in the 800 μm device to 143.1 μA in the 1000 μm device. The sensitivity of these devices was also analyzed, and it was found that the sensitivity of both devices was highly linear

across a current change of 2 orders of magnitude. Additionally, the GaN LED I-V curve also showed high linearity in its forward voltage as the temperature increased, similar to that of the heterojunction I-V curves. All of these results point to the application of heterojunctions for high power optocoupler applications as well as their use as temperature sensors in harsh environments.

5.2 Optical Characterization of InGaN/GaN Multi-Quantum Well

The MQW InGaN/GaN structure subject to PL spectroscopy showed great potential for its integration into high temperature optoelectronics. It was observed that as the temperature increased, there was redshift indicating the decrease in bandgap. The intensity of this MQW device is analyzed at temperatures ranging from 10K to 800K. Since this structure showed a small, gradual decrease in bandgap, it shows promise for its use in high temperature applications. Additionally, this InGaN/GaN MQW structure has been reported to have a 44% quantum efficiency at 800K [23], further emphasizing its potential for high temperature applications.

5.3 Future Work

Now that these wide bandgap heterostructures and MQW structures have shown their capability of operating at elevated temperatures, further analyzing their PL measurements, studying its detector response, and the reliability and lifetime of these wide bandgap LEDs are important to know and understand in order for them to be fully integrated into these high power, high temperature power modules.

To further characterize this material, this InGaN/GaN MQW structure can also be characterized through PL spectroscopy using different pumping powers to analyze its effects on the light intensity over a wide range of temperature. Furthermore, other samples with wider and narrower bandgaps can be subjected to these PL measurements. By doing so, it can be observed

how the bandgap changes at elevated temperatures with wider and narrower room temperature bandgaps. To compliment these results, analyzing the quantum efficiency versus temperature of these structures will give insight into which materials are able to potentially operate at these elevated temperatures.

Additionally, further studies need to be conducted into the packaging of these LED devices and optocoupler, pushing their melting point limits beyond those of operation. Once these parameters and goals are understood and met, the integration of these LEDs will be possible.

References

[1] P. G. Neudeck, R. S. Okojie, and Liang-Yu Chen, "High-temperature electronics - a role for wide bandgap semiconductors?," *Proc. IEEE*, vol. 90, no. 6, pp. 1065–1076, Jun. 2002.

[2] R. R. Schaller, "Moore's law: past, present and future," *IEEE Spectr.*, vol. 34, no. 6, pp. 52–59, Jun. 1997.

[3] C. Buttay *et al.*, "State of the art of high temperature power electronics," *Mater. Sci. Eng. B*, vol. 176, no. 4, pp. 283–288, Mar. 2011.

[4] J. B. Casady and R. W. Johnson, "Status of silicon carbide (SiC) as a wide-bandgap semiconductor for high-temperature applications: A review," *Solid. State. Electron.*, vol. 39, no. 10, pp. 1409–1422, Oct. 1996.

[5] R. J. Valentine, "Power module control design," in *IAS '95. Conference Record of the 1995 IEEE Industry Applications Conference Thirtieth IAS Annual Meeting*, vol. 1, pp. 904–910.

[6] R. Kliger, "Integrated transformer-coupled isolation," *IEEE Instrum. Meas. Mag.*, vol. 6, no. 1, pp. 16–19, Mar. 2003.

[7] R. W. Johnson, J. L. Evans, P. Jacobsen, J. R. R. Thompson, and M. Christopher, "The Changing Automotive Environment: High-Temperature Electronics," *IEEE Trans. Electron. Packag. Manuf.*, vol. 27, no. 3, pp. 164–176, Jul. 2004.

[8] T. P. Chow and R. Tyagi, "Wide bandgap compound semiconductors for superior high-voltage unipolar power devices," *IEEE Trans. Electron Devices*, vol. 41, no. 8, pp. 1481–1483, 1994.

[9] K. C. Sedra, Adel S.; Smith, *Microelectronic Circuits Sedra Smith 7th Edition*, 7th ed. Oxford University Press, 2015.

[10] University of Warwick, "Light Emitting Diodes," *Department of Physics*, 2011. [Online]. Available: https://warwick.ac.uk/fac/sci/physics/current/postgraduate/regs/mpagswarwick/ex5/devices/led/. [Accessed: 02-May-2018].

[11] E. Polyutina, "Light Emitting Diodes (LEDs): A Look Inside." [Online]. Available: http://asdn.net/asdn/physics/leds.php. [Accessed: 02-May-2018].

[12] Steven Keeping, "Whiter, Brighter LEDs," *DigiKey*, 2011. [Online]. Available: https://www.digikey.sg/en/articles/techzone/2011/aug/whiter-brighter-leds. [Accessed: 27-Apr-2018].

[13] M.-H. Chang, D. Das, P. V. Varde, and M. Pecht, "Light emitting diodes reliability review," *Microelectron. Reliab.*, vol. 52, no. 5, pp. 762–782, May 2012.

[14] J. Hu, L. Yang, and M. W. Shin, "Electrical, optical and thermal degradation of high power GaN/InGaN light-emitting diodes," *J. Phys. D. Appl. Phys.*, vol. 41, no. 3, p. 035107, Feb. 2008.

[15] S. Madhusoodhanan, S. Sandoval, Y. Zhao, M. E. Ware, and Z. Chen, "A Highly Linear Temperature Sensor Using GaN-on-SiC Heterojunction Diode for High Power Applications," *IEEE Electron Device Lett.*, vol. 38, no. 8, pp. 1105–1108, Aug. 2017.

[16] J. Melorose, R. Perroy, and S. Careas, *Nanoscale Science and Tecnology*, vol. 1. 2015.

[17] S. Perkowitz, *Optical characterization of semiconductors : infrared, Raman, and photoluminescence spectroscopy*. Academic Press, 1993.

[18] S. Perkowitz ', D. G. Seller, and W. M. Duncan, "Optical Characterization in

Microelectronics Manufacturing," *J. Res. Natl. Inst. Stand. Technol. Res. Natl. Inst. Stand. Technol*, vol. 99, no. 99.
[19] M. Mansoor, I. Haneef, S. Akhtar, A. De Luca, and F. Udrea, "Silicon diode temperature sensors—A review of applications," *Sensors Actuators A Phys.*, vol. 232, pp. 63–74, Aug. 2015.
[20] C. Yao *et al.*, "Electromagnetic noise coupling and mitigation for fast response on-die temperature sensing in high power modules," in *2016 IEEE Applied Power Electronics Conference and Exposition (APEC)*, 2016, pp. 1554–1560.
[21] E. R. Motto and J. F. Donlon, "IGBT module with user accessible on-chip current and temperature sensors," in *2012 Twenty-Seventh Annual IEEE Applied Power Electronics Conference and Exposition (APEC)*, 2012, pp. 176–181.
[22] H. Ichikawa, T. Ichimura, and S. Soyano, "IGBT Modules for Hybrid Vehicle Motor Driving," *Fuji Electr. Rev*, vol. 55, no. 2, pp. 46–50.
[23] A. Sabbar, S. Madhusoodhanan, and et al, "Investigation of High Temperature Photoluminescence Efficiency from InGaN/GaN MQWs." CLEO 2018.
[24] S. Santra, P. K. Guha, S. Z. Ali, I. Haneef, F. Udrea, and J. W. Gardner, "SOI diode temperature sensor operated at ultra high temperatures - a critical analysis," in *2008 IEEE Sensors*, 2008, pp. 78–81.
[25] Y. P. Varshni, "Temperature dependence of the energy gap in semiconductors," *Physica*, vol. 34, no. 1, pp. 149–154, Jan. 1967.